In Vivo and in Vitro Proteome Analysis of Human Immunodeficiency Virus (HIV)-1-infected, Human CD4+ T Cells

Nemeth, J., Vongrad, V., Metzner, K. J., Strouvelle, V. P., Weber, R., Pedrioli, P., ... Collins, B. C. (2017). In Vivo and in Vitro Proteome Analysis of Human Immunodeficiency Virus (HIV)-1-infected, Human CD4+ T Cells. Molecular and Cellular Proteomics, 16(4 suppl 1), S108-S123. https://doi.org/10.1074/mcp.M116.065235

Published in:
Molecular and Cellular Proteomics

Document Version:
Publisher's PDF, also known as Version of record

Research

In Vivo and *in Vitro* Proteome Analysis of Human Immunodeficiency Virus (HIV)-1-infected, Human CD4$^+$ T Cells*[S]

Johannes Nemeth‡§¶, Valentina Vongrad‡‖, Karin J. Metzner‡‖, Victoria P. Strouvelle‡‖, Rainer Weber‡, Patrick Pedrioli§, Ruedi Aebersold§, Huldrych F. Günthard‡‖‡‡, and Ben C. Collins§‡‡§§**

Host-directed therapies against HIV-1 are thought to be critical for long term containment of the HIV-1 pandemic but remain elusive. Because HIV-1 infects and manipulates important effectors of both the innate and adaptive immune system, identifying modulations of the host cell systems in humans during HIV-1 infection may be crucial for the development of immune based therapies. Here, we quantified the changes of the proteome in human CD4$^+$ T cells upon HIV-1 infection, both *in vitro* and *in vivo*. A SWATH-MS approach was used to measure the proteome of human primary CD4$^+$ T cells infected with HIV-1 *in vitro* as well as CD4$^+$ T cells from HIV-1-infected patients with paired samples on and off antiretroviral treatment. In the *in vitro* experiment, the proteome of CD4$^+$ T cells was quantified over a time course following HIV-1 infection. 1,725 host cell proteins and 4 HIV-1 proteins were quantified, with 145 proteins changing significantly during the time course. Changes in the proteome peaked 24 h after infection, concomitantly with significant HIV-1 protein production. In the *in vivo* branch of the study, CD4$^+$ T cells from viremic patients and those with no detectable viral load after treatment were sorted, and the proteomes were quantified. We consistently detected 895 proteins, 172 of which were considered to be significantly different between the viremic patients and patients undergoing successful treatment. The proteome of the *in vitro*-infected CD4$^+$ T cells was modulated on multiple functional levels, including TLR-4 signaling and the type 1 interferon signaling pathway. Perturbations in the type 1 interferon signaling pathway were recapitulated in CD4$^+$ T cells from patients. The study shows that proteome maps generated by SWATH-MS indicate a range of functionally significant changes in the proteome of HIV-infected human CD4$^+$ T cells. Exploring these perturbations in more detail may help identify new targets for immune based interventions. ***Molecular & Cellular Proteomics 16: 10.1074/mcp.M116.065235, S108–S123, 2017.***

Therapeutic approaches against HIV-1 are mired in dichotomy. On the one hand, drugs targeting the virus are turning HIV infection successfully into a therapeutically manageable chronic disease, blocking transmission and increasing survival dramatically (1). On the other hand, host-targeted approaches such as vaccines or attempts to repair or boost the immune system failed without exception (2, 3). However, it is generally assumed that vaccines and sterilizing treatment are prerequisites to eradicate HIV-1, because lifelong treatment is difficult to implement, costly, and has side effects (4).

Current antiretroviral therapy stops viral replication but cannot kill latently infected cells. Therefore, other approaches are needed that can reverse HIV-1 latency or increase innate or adaptive immune responses to kill latently infected cells. Because the virus requires host cells for replication and survival, it needs to interact and modify the host environment to its advantage. Although these complex interactions have been extensively studied on a transcriptional level (5, 6), the knowledge about the changes on the protein level are sparse (7, 8). Therefore, more knowledge on the effects of HIV-1 on host proteome networks in human cells infected by the virus is needed to better understand virus-host interactions. It has been estimated that genetic determinants of the virus are responsible for 30–50% of the variability of the viral set point, a surrogate marker for disease progression and compared with 20% of the host genome (9). Thus, exploring host networks in clinically well characterized human individuals infected with HIV-1 is crucial for the advancement of host-targeted therapies (10). On a transcriptome level, the networks of HIV-1-infected CD4$^+$ T cells have already been studied both *in vitro* (5) and *in vivo* (11, 12). However, the changes detectable on the transcriptome level are largely

From the ‡Division of Infectious Diseases and Hospital Epidemiology, University Hospital Zurich, University of Zurich, Zurich 8091; §Department of Biology, Institute of Molecular Systems Biology, ETH Zurich, Zurich CH-8093; **Faculty of Science, University of Zurich, Zurich 8057; and ‖Institute of Medical Virology, University of Zurich, Zurich 8057, Switzerland

Received November 1, 2016 and in revised form, February 3, 2017
Published, MCP Papers in Press, February 21, 2017, DOI 10.1074/mcp.M116.065235

Author contributions: J. N., K. J. M., R. A., H. G., and B. C. C. designed research; J. N., V. V., V. S., P. P., and B. C. C. performed research; B. C. C. contributed new reagents or analytic tools; J. N., K. J. M., P. P., R. A., H. G., and B. C. C. analyzed data; J. N., K. J. M., R. W., P. P., R. A., H. G., and B. C. C. wrote the paper.

TABLE I
Patient characteristics

Patient IDs	Treatment	Viral load, copies/ml	CD4/mm^3	% CD4	CD8/mm^3	% CD8
1	off	81,800	486	20	1,155	48
	on	<20	517	17	1,505	49
2	off	144,000	391	24	809	51
	on	<20	359	26	644	47
3	off	32,500	440	20	1,371	61
	on	<20	477	40	463	39
4	off	2,370	478	36	611	46
	on	<20	503	41	478	39
5	off	996,000	420	35	546	46
	on	<20	793	56	294	21
6	off	38,300	376	24	842	54
	on	<20	668	29	1,075	47
7	off	29,000	476	31	709	46
	on	<20	667	35	638	34
8	off	3,510	462	30	616	40
	on	<20	582	24	739	31
9	off	110,000	614	31	1,097	56
	on	<20	692	36	911	47
10	off	27,100	602	34	826	47
	on	<20	758	46	551	33

driven by viral replication. Therefore, they are not ideal for the discovery of mechanisms of viral control (11). In contrast, proteins are the main molecular effectors of the cell and are at the functional interface between virus and host. Analysis of the proteome may therefore be useful to detect new mechanisms associated with control of the virus.

Mass spectrometry (MS) has increasingly become the method of choice for analysis of complex protein samples, both qualitatively and quantitatively (13). We have recently developed SWATH-MS, a technique that combines the high quantitative accuracy of targeted proteomics with the broader coverage achievable with discovery proteomics. In essence, SWATH-MS is a massively parallel targeted mass spectrometric strategy that requires the *a priori* generation of spectral libraries that are then used to identify and quantify query peptide in the acquired datasets (14, 15). SWATH-MS provides selected reaction monitoring-like performance in terms of reproducibility, quantitative accuracy, data completeness, and dynamic range (16). Furthermore, and unlike selected reaction monitoring, SWATH-MS can quantify an unlimited number of target peptides as long as they have been previously observed by DDA[1] (15).

MS approaches have been used previously to quantify the changes in the proteome of T cell lines and macrophages upon infection with HIV-1 (7, 8). However, the proteome of the main target cell of HIV-1, the human CD4$^+$ T cell, has not been assessed yet.

In this study, we describe the results of the exploratory study in which the proteome of human CD4$^+$ T cells, the most important target cell for HIV-1, is quantified to detect the changes associated with HIV-1 infection. By infecting human CD4$^+$ T cells *in vitro* and following the effects of the infection on the host proteome over time and by assessing the proteome differences in paired samples from viremic and subsequently treated patients with no detectable viral load, we aimed to cover the changes of the CD4$^+$ T cell proteome associated with HIV-1 infection in both *in vitro* and in human individuals. The data re-iterate the central role for type 1 interferon during HIV-1 infection and suggest a possibly novel role for TLR-4 signaling. Finally, the changes in the proteome during *in vitro* and the *in vivo* HIV infection are to large extent dissimilar, except for significant enrichment of type 1 interferon signaling upon functional enrichment analysis.

PATIENTS AND METHODS

Patients—10 HIV-1-infected individuals were enrolled from the longitudinal Zurich Primary HIV-1 Infection Study (ZPHI), which is an open label, non-randomized, observational, single-center study (www.clinicaltrials.gov, ID 5 NCT00537966) (17). Blood samples at two different time points of each patient were investigated. At time point 1, the patients were not treated and had HIV-1 detectable. At time point 2, the patients were treated and had no detectable viral load for a minimum of 6 months. For patient details, see Table I.

Ethics Statement—The ethic committee of the University Hospital Zurich approved the study protocol and a written informed consent was obtained from all patients. Buffy coats from healthy donors were received from the Blood Donation Service Zurich, Swiss Red Cross, Switzerland. Written in-

[1] The abbreviations used are: DDA, data-dependent acquisition; ZPHI, Zurich Primary HIV-1 Infection Study; PBMC, peripheral blood mononuclear cell; m.o.i., multiplicity of infection; ACN, acetonitrile; FA, formic acid; TPP, tripeptidyl-peptidase.

formed consent was obtained for the use of buffy coats for science, which were not needed for medical purposes by the Blood Donation Center.

CD4$^+$ T Cell Culture and Infection—Peripheral blood mononuclear cells (PBMCs) were isolated from buffy coats, as described previously (18), and enriched for CD4$^+$ T cells by magnetic microbeads according to the manufacturer's protocol (Miltenyi Biotec). After a three-way stimulation (phytohemagglutinin 5.0 μg/ml, phytohemagglutinin 0.5 μg/ml, and Oct3) for 3 days, the cells were infected with HIV-1$_{JR-FL}$ by spinoculation for 2 h at 1,200 $\times$ *g* at a multiplicity of infection (m.o.i.) of 1 (19). After infection, the cells were washed twice in PBS and cultured in RPMI 1640 media containing penicillin/streptomycin, 10% FCS, and 50 units of IL-2/ml. Supernatant for p24 ELISA was collected 0, 12, 24, and 48 h post-infection. The time points were chosen to allow the virus to finish a full infectious circle (5). CD4$^+$ T cell purity was confirmed by flow cytometry, ranging between 96.3 and 99.8%. The HIV-1$_{JR-FL}$ virus stock was generated by transfection of 293 T cells with pJR-FL and titrated on PBMCs (18).

Cryopreserved PBMC Procedures—Cryopreserved PBMCs were thawed in a 36 °C water bath and were washed twice with PBS at room temperature. 1 $\times$ 10^6 cells were lysed immediately, and the remaining cells were positively selected using magnetically labeled CD4 and CD8 microbeads and subsequent column purification according to the manufacturer's protocol (Miltenyi Biotec). CD4$^+$ T cell purity, verified by flow cytometry, was 97.8% (96.3–99%) (median (range).

Experimental Design and Statistical Rationale—For the *in vitro* infection experiment, each time point, including controls, was performed in triplicate. Each sample represents a biological replicate. For the MapDIA statistical model, three biological replicates were sufficient. For the human samples, a total of 10 patient's samples were obtained. Two patients were excluded due to low cell numbers. Therefore, a total of eight patients were measured at each time point, representing a biological replicate each. We were able to maintain the Replicate Design Model, which enabled us to use the MapDIA statistical model despite the exclusion of two samples.

Proteomics Sample Preparation—Approximately 1 $\times$ 10^6 cells were washed with PBS and resuspended in lysis buffer containing 1.2% sodium deoxycholate monohydrate in 50 mM ammonium bicarbonate buffer (150 μl per 1 $\times$ 10^6 cells). The cell suspension was thoroughly vortexed and incubated at room temperature for 10 min while shaking at 1,000 rpm. Subsequently, cells were subjected to three 10-min cycles of sonication at 4 °C (100% output, 50% intervals, Branson Sonifier 450, Emerson).

Ice-cold acetone (−20 °C) was added to the lysate at a rate of 6 volumes to 1 volume of lysate and incubated for 1 h on ice. The cell lysate was centrifuged for 15 min at full speed at 4 °C, washed another three times with ice-cold acetone, and then allowed to dry completely. The proteins were resuspended in 8 M urea, 100 mM ammonium bicarbonate buffer. The protein concentration was estimated using the BCA assay (Pierce). From each sample only 50 μg of protein was used for subsequent steps. Protein disulfide bonds were reduced by adding 5 mM tris(2-carboxyethyl)phosphine and incubating for 30 min at 30 °C. Free cysteine residues were alkylated by adding 40 mM iodoacetamide and incubating for 60 min in the dark at room temperature. Subsequently, the samples were diluted with 0.05 M ammonium bicarbonate buffer to a urea concentration of $<$2 M, and 1 μg of sequencing grade modified trypsin was added (w/w 1:50). The samples were incubated overnight at 30 °C with shaking at 300 rpm. To stop the tryptic digest, the pH was lowered to 2 using trifluoroacetic acid (final concentration of ~1%) followed by an incubation for 30 min at 37 °C with shaking at 500 rpm.

The cleared peptide solution was desalted with C18 MicroSpin columns (The Nest Group, 5–60 μg loading capacity). Prior to use, the C18 columns were activated with 100% methanol, followed by 80% acetonitrile (ACN), 0.1% TFA, followed by equilibration with 2% ACN, 0.1% TFA. After loading, the columns were washed with 2% ACN, 0.1% TFA. Subsequently, the peptides were eluted with 40% ACN, 0.1% TFA, dried under vacuum, resolubilized in 2% ACN, 0.1% FA, and added at 1:20 with iRT peptides (Biognosys).

Spectral Library and SWATH Peptide Query Parameter Generation—The spectral library and SWATH peptide query parameters were generated essentially as described (20). The TripleTOF 5600 mass spectrometer (AB Sciex) was coupled to a nanoLC 1Dplus system (Eksigent), and the chromatographic separation of the peptides was performed on a 20-cm emitter (75 μm inner diameter, New Objective) packed in-house with C18 resin (Magic C18 AQ 3 μm diameter, 200 Å pore size, Michrom BioResources). A linear gradient from 2 to 35% solvent B (solvent A, 2% ACN, 0.1% FA; solvent B, 98% ACN, 0.1% FA) was run over 120 min at a flow rate of 300 nl/min. The mass spectrometer was operated in IDA mode with a 500-ms survey scan from which up to 20 ions exceeding 250 counts/s were isolated with a quadrupole resolution of 0.7 Da, using an exclusion window of 20 s. Rolling collision energy was used for fragmentation, and an MS2 spectrum was recorded after an accumulation time of 50 ms. Raw data files (wiff) were centroided and converted into mzML format using the AB Sciex converter (beta version 2011) and subsequently converted into mzXML using openMS (version 1.8). The converted data files were searched using the search engines X!Tandem (*k*-score, version 2013.06.15.1) and Comet (version 2013.02, revision 2) against the UniProt-SwissProt complete proteome for *Homo sapiens* (canonical sequences) with the protein sequences derived from full-length consensus sequences of viral RNA genome of both the HIV-1$_{JR-FL}$ strain used for the *in vitro* infection model and the viral RNA sequences of 8–10 patients (HIV_fasta_file.txt, supplemental material) (21). The enzyme specificity was set to fully tryptic with two missed cleavages allowed. In total, the database contained 20,149 target sequences and 20,117 decoy se-

quences. The tolerated mass errors were 50 ppm on MS1 level and 0.1 Da on MS2 level. Carbamidomethylation of cysteines was defined as a fixed modification and methionine oxidation as a variable modification. The search results were processed with PeptideProphet and iProphet as part of the TPP 4.7.0. The spectral library was constructed from the iProphet results with an iProphet probability cutoff of 0.98422, corresponding to a 1% FDR on a protein level as determined by Mayu (version 1.08). The raw and consensus spectral libraries were built with SpectraST (version 5.0) using the -cICID_QTOF option for high resolution and high mass accuracy and -c_IRT and -c_IRR options to normalize all retention times according to the iRT peptides with a linear regression. The six most intense y and b fragment ions of charge state 1 and 2 were extracted from the consensus spectral library using spectrast2tsv.py from msproteomicstools (https://pypi.python.org/pypi/msproteomicstools). Fragment ions falling into the swath window of the precursor were excluded as there is often interference with the resulting signals. Decoy transition groups were generated based on shuffled sequences (decoys similar to targets were excluded) by the OpenMS tool OpenSwathDecoyGenerator (version 1.10.0) and appended to the final SWATH library in TraML format (20).

SWATH Data Acquisition—TripleTOF 5600 mass spectrometer was set up as described above but operated in SWATH mode using the following parameters. For liquid chromatography, a linear gradient from 2 to 35% solvent B (98% ACN, 0.1% FA) was run over 120 min at a flow rate of 300 nl/min (patient samples) or 5–30% over 60 min (*in vitro* infections). Acquisition of a 250-ms survey scan was followed by acquisition of 64 fragment ion spectra from 64 precursor isolation windows (swaths) with variable width chosen to minimize precursor ion density in each window (16). The swaths were overlapping by 1 *m/z* and covered a range of 400–1200 *m/z*. The SWATH MS2 spectra were recorded with an accumulation time of 50 ms and cover 100–2000 *m/z*. The collision energy for each window was determined according to the calculation for a charge 2+ ion centered upon the window with a spread of 15. Raw data files (wiff) were converted into mzXML format using ProteoWizard as described (14).

SWATH Data Analysis with OpenSWATH—The SWATH data were analyzed using OpenSWATH version 1.10 with the following parameters. Chromatograms were extracted with 0.05 *m/z* around the expected mass of the fragment ions and with an extraction window of ±5 min around the expected retention time after iRT alignment. The best model to separate true from false positives (per run) was determined by pyprophet with 10 cross-validation runs. The runs were subsequently aligned using TRIC as described with a target FDR of 0.01 (22).

Relative Protein Quantification—To obtain fold changes and corresponding *p* values of all proteins compared with the time-matched uninfected controls for *in vitro* infections, or non-viremic patient samples, the software MapDIA was used. Median normalization was applied prior to analysis by MapDIA throughout. A model-based statistical significance analysis of protein level differential expression between the groups of interest was performed as described in the MapDIA package. iRT peptides and serum proteins (samples were stored in BSA containing buffer) were removed from the analysis (supplemental Fig. 1).

Protein Abundance Estimation—For label-free abundance estimations of all proteins identified by SWATH MS, the aLFQ package was used (23). Protein abundances were computed as the sum of the top five most intense fragment ions from the three most intense peak groups. The TRIC strategy for automated peptide alignment was used (22). Requantified values were used when no reliable signal was found. A protein had to be detected for a minimum of three times per group in order for the remaining values to be requantified and considered for downstream analysis.

Clustering, Functional Annotation, and Network Analysis—Clustering was performed using the heatmap2 function in R. For functional annotation, the ClueGO app for Cytoscape was used (24). An Enrichment/Depletion method with a two-sided hypergeometric test was applied, correcting with a Bonferroni step down correction. Min GO level was set to 4 and Max GO level to 10. The protein list from the spectral library was used as background throughout. For networks based on STRING, an evidence grade cutoff of 0.4 was used.

RESULTS

Qualitative Characterization of the HIV-1 and Host Cell Proteomes—CD4$^+$ T cells from blood donors were isolated and infected *in vitro* with HIV-1$_{JR\text{-}FL}$(18). The study approach is summarized in Fig. 1*A*. The HIV-1 protein p24 was quantified by ELISA in the supernatant to confirm successful infection (Fig. 1*B*). Because human CD4$^+$ T cells need to be activated for successful infection with HIV-1 *in vitro*, we focused our analysis on the log2 fold changes between paired infected and uninfected cells at a given time point. To generate a spectral library for use as reference in generating peptide query parameters for the peptide-centric analysis of SWATH-MS data, we performed DDA analysis of the proteomes of *in vitro* HIV-1-infected human CD4$^+$ T cells as well as sorted CD4$^+$ T cells, CD8$^+$ T cells, and PBMC from HIV-1-infected individuals (Fig. 1*A* and supplemental Fig. 2) following our published protocol (20). We added the sequence of HIV-1$_{JR\text{-}FL}$ used for *in vitro* infection as well as eight full-length HIV-1 sequences from patients to our protein sequence database. This resulted in a reference spectral library (Fig. 1*A*, qualitative MS), consisting of 3,360 proteins based on 22,901 peptides with an FDR of 1% on the protein level, including four HIV-1 proteins: Env_gp120; Nef; matrix protein (p17); and capsid protein (p24) (Table II, HIV_fasta_file.txt). Using DDA mode for the library creation, we were able to detect HIV-1 proteins from *in vitro* experiments only, despite adding the matching HIV-1 sequence of the individual virus of each pa-

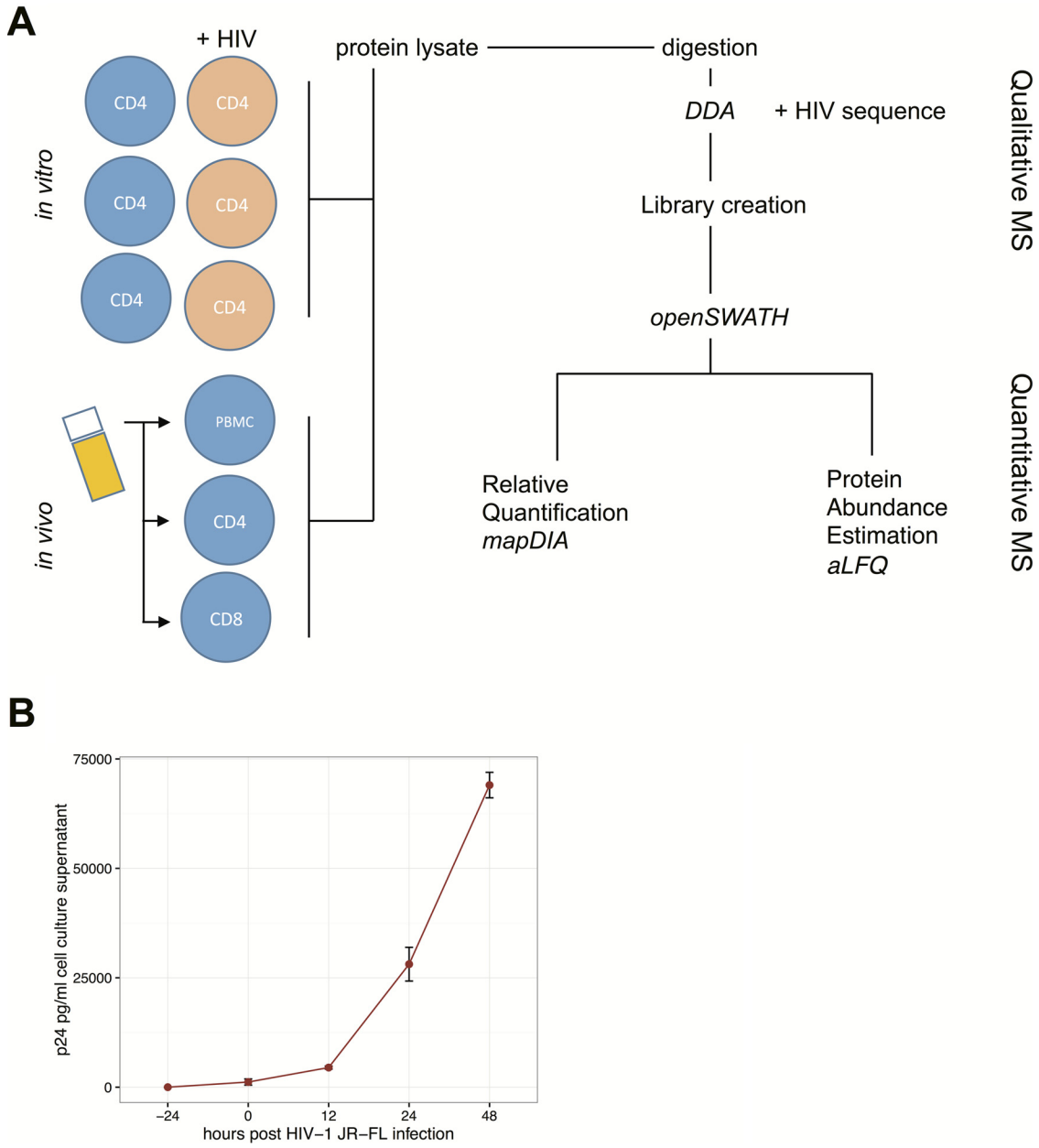

FIG. 1. **Experimental design.** *A,* lysates from human CD4+ T cells as well as PBMC, sorted CD4+ T cells, and sorted CD8+ T cells were used to generate a spectral library and HIV-1 sequences (qualitative MS). Using this library, both relative changes between the samples of interest as well as protein abundance (quantitative MS) were calculated using the mapDIA and the aLFQ package, respectively. *B,* p24 in the cell culture supernatant from infected CD4+ T cells as detected by ELISA.

tient from 8 of the 10 patients. Overall, it is not very surprising that we were unable to find viral proteins in human individuals, given that even in actively replicating patients 1 of ~617–771 of CD4+ T cells is productively infected, *i.e.* produces viral protein (25). In contrast, after spinoculation with an m.o.i. of 1, close to 100% of CD4+ T cells are infected *in vitro*.

Changes in the Proteome of in Vitro HIV-1-infected CD4+ T Cells over Time—To determine the changes of the proteome associated with HIV-1 infection, we measured quantitative proteome profiles of CD4+ T cells infected *in vitro* with HIV-1 by SWATH-MS. Of 1,725 proteins (1% FDR) consistently quantified during the time course, a total of 145 unique proteins (8%) were significantly different between infected and uninfected CD4+ T cells according to a differential protein expression analysis using a Bayesian hierarchical model as implemented in mapDIA (26), using a threshold of (FDR <0.05 and log2 fold changes >1 and < -1) (supplemental Table 1). The most profound changes in the proteome were detectable 24 h after infection (Fig. 2*A*). To assess the overall structure of the changes in the proteome, we performed hierarchical clus-

TABLE II
HIV proteins

Viral protein	Function	Seq. coverage (%)	distinct peptides
Env_gp120	Part of gp160, binds to CXCR4/CCR5	7.4	3
Nef	Early protein, inhibits T cell activation	11.1	2
P17	Part of GAG, structural protein	36.9	13
P24	Capsid, forms conical core of virions	18.0	4

tering of differentially expressed proteins. We were able to detect four high level clusters over the time course. Compared with uninfected CD4$^+$ T cells, clusters of down-regulated proteins were most prominent. To illustrate the dynamics of the four clusters, we plotted all the traces of each cluster and, additionally, selected proteins from each cluster (Fig. 3). To assess the changes in the proteome and the structure of the clusters on a functional level, we applied Gene Ontology (GO) term enrichment analysis to the different clusters (24). The *blue cluster a* (Fig. 2*B*) contains 30 proteins and displayed a biphasic trace with up-regulation at time point of 24 h and down-regulation at time point of 48 h (Fig. 3*A*).

Cluster a in *blue* (Fig. 3*A*) contained TPP-1. Functional enrichment analysis showed significant enrichment of serine endopeptidase activity, cysteine endopeptidase activity, and symporter and phosphatase activity (Fig. 4*A* and supplemental Table 2).

Cluster b in *turquoise* consists of 25 proteins (Fig. 2*B*), which are down-regulated over the course of infection (Fig. 3*B*). There was no enrichment of GO terms detectable for this cluster. *Cluster b* contains the protein phosphatase 3 catalytic subunit α (PPP3CA), a calmodulin-stimulated protein phosphatase (Fig. 3*B*).

Cluster c contains 27 proteins, and they are marked in *olive green* (Fig. 2*B*). The overall trace displays an early down-regulation of proteins after 12 h after infection (Fig. 3*C*). GO term enrichment analysis revealed one significantly enriched functional term, transcription corepressor activity. Cluster c contains TRNA methyltransferase 11–2 (TRMT 112), which is involved in the methylation of tRNA and proteins (Fig. 2*C*).

Cluster d in *red* (Fig. 2*B*) is the largest cluster with a total of 63 proteins (Fig. 2*B*). The general trace displays down-regulation of proteins after 24 h (Fig. 3*D*). The single protein shows protein S100-A8, which belongs to the group myeloid-related proteins After a three-way stimulation (phytohemagglutinin 5.0 μg/ml, phytohemagglutinin 0.5 μg/ml, and Oct3) for 3 days, (Fig. 3*D*). Functional enrichment analysis showed significant enrichment of multiple GO terms, including TLR-4 binding, type 1 interferon signaling pathways, nucleosome binding, endopeptidase inhibitor activity, and ribonucleotide diphosphatase reductase activity (Fig. 4*B* and supplemental Table 2). In sum, we can re-capitulate the dynamics of single proteins known to be important during HIV infection in the context of the changing proteome.

We attempted to correlate our differential proteome data with gene expression data from a previous study (5); however, no significant correlation of the log2 fold change *versus* uninfected controls for transcripts and protein could be found (supplemental Fig. 3). Although the infection experiment in this paper was similar, there were significant differences, particularly with respect to the host cell line used (T cell line in the cited transcript study as opposed to primary CD4$^+$ T cells in our experiment). The lack of correlation may also reflect the complex dynamics of the infection system and the temporal difference in protein and transcript responses, but to address this, a study designed specifically to address this would be required.

Abundance and Dynamics of Viral Proteins—In this section, we aimed to measure HIV proteins within the host proteome. For the quantification of viral proteins, the protein abundances were determined by best flyer peptide approach (27) using the aLFQ package (23). In *in vitro* HIV-1-infected CD4$^+$ T cells, the production of the intracellular viral protein peaked at 24 h with a swift decrease at 48 h (Fig. 4*A*). The most prominent changes in the human proteome occurred simultaneously, peaking at time point 24 h (Fig. 1*A*). All four HIV-1 proteins measured displayed highly synchronous dynamics. To depict the abundance of viral proteins in the context of the host proteome, we plotted those abundances in the context of the host proteins at 24 h and highlighted host proteins associated with the GO group "viral defense" (Fig. 4*B*). Within 24 h, absolute viral protein quantities match constitutively expressed proteins like CD4.

It is noteworthy that the proteins detected after 24 h are all structural proteins except for NEF. This is in line with the observation that HIV-1 completes the viral cycle at this time point (5). Therefore, it is not surprising to detect proteins that are consistent with an intact virus, like p17, a matrix protein with immune modulatory capacity. NEF remained highly expressed at this time point, in absolute quantities close to the amount of CD4. The inhibitory activity of NEF on CD4 is well established (28). Hence, these data suggest that the immune modulatory protein NEF remains to be expressed at high levels despite the successful production of late viral proteins. Indeed, NEF induces a massive secretory state not only in HIV-1-infected cells but also bystander cells (29). Therefore, it is suggestive that the massive production of NEF together with intact virus at time point 24 h is likely to facilitate subsequent infections.

Changes in the Proteome of CD4$^+$ T Cells from Patients Are Associated with HIV-1 Viremia—Next, we tried to determine whether any of the changes observed in the *in vitro* HIV-1

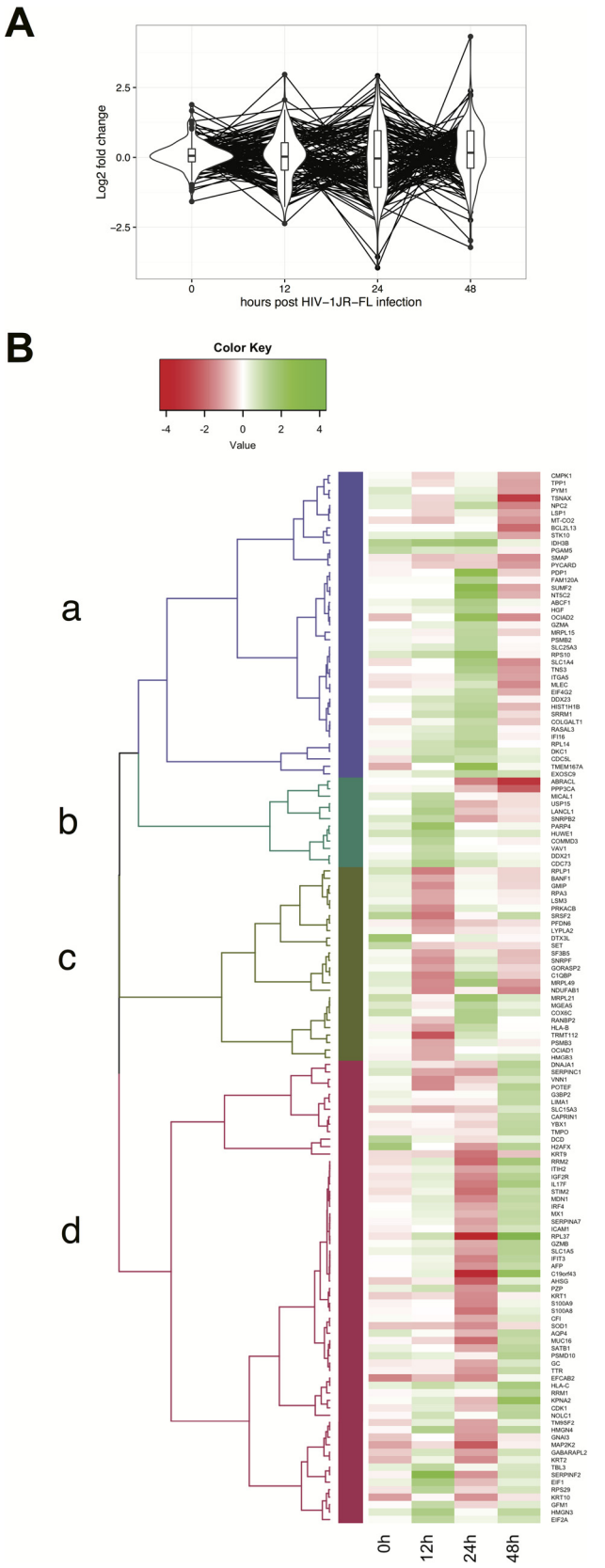

infection model are recapitulated in CD4+ T cells from HIV-1-infected individuals. Samples were collected from patients participating in the longitudinal Zurich Primary HIV-1 Infection Study. Samples were obtained from patients during viremia as well as at least 6 months after successful antiretroviral treatment where no viral load was detectable (Table I). Therefore, we cannot exclude that the medication itself contributes to the observed changes of the proteome. The clinical samples were heterogeneous in terms of absolute protein yield extracted due to low cell numbers after sorting. Samples with too low amounts of cells were excluded pairwise to retain the Replicate Design Model. We were unable to link to any specific pattern, such as prolonged storage, probably due to the limited sample number. In total, we were able to measure the proteome in two time points each from CD4+ T cells of eight individual patients, and we were able to consistently measure 895 proteins in CD4+ T cells. Next, we compared the quantitative changes in CD4+ T cells in patients during HIV-1 viremia and after successful therapy. Overall, the changes were not very pronounced in terms of log2 fold changes (Fig. 5*A*). Because CD4+ T cells are the main population of infected cells in peripheral blood, it is to be expected that this cell population shows the biggest changes upon treatment. Using an FDR cutoff of 1% and log2 fold changes of <0.5 to >0.5, as threshold for significance, 57 proteins were up-regulated, and 115 were down-regulated in CD4+ T cells. After functional enrichment analysis, the GO terms RNA polymerase II core promoter, type 1 interferon signaling, neutrophil killing of a symbiont cell, and antigen presentation were enriched in up-regulated proteins (Fig. 5*B* and supplemental Table 2). Specifically, the small ubiquitin-like protein-modified interferon-stimulated gene 15 (ISG)-15 plays an important role by inhibiting the release of HIV-1 particles (30), and correlates with viral load in humans (31). The rather unexpected finding of increased syntaxin-binding protein (STXBP)-2 is in line with findings in a Jurkat T cell line, showing that STXBP-2 is a strong inhibitor of retroviral transcription (32). RuvB-like 2 (RVB2), an ATP-dependent DNA helicase, is exploited by HIV-1 to retain the correct ratio of the HIV-1-1 structural protein Gag to the envelope protein Env; in addition, RVB2 levels correlate with HIV load in humans (33). The detection of the proteins TAP-1 and TAP-2 suggests that there is a contamination of CD4+ T cells with dendritic cells. Dendritic cells

FIG. 2. **Changes in the proteome of *in vitro* HIV-1-infected CD4+ T cells over time.** *A,* violin plots of log2 fold changes of proteins at given time points comparing HIV-1-infected *versus* -uninfected CD4+ T cells. Single proteins are connected by *lines*. *Box plots* show mean ± S.E. An FDR <0.05 and log2 fold changes >1 and <-1 after adjusting for multiple testing were considered significant. The model-based statistical significance analysis from the mapDIA package was used for statistical analysis. *B,* heat map displaying log2 fold changes of proteins changing at least once significantly (FDR <0.05 and log2 fold changes >1 and <-1) during the time course. Four high level clusters are highlighted in *blue* (*a*), *green* (*b*), *olive* (*c*), and *red* (*d*), respectively.

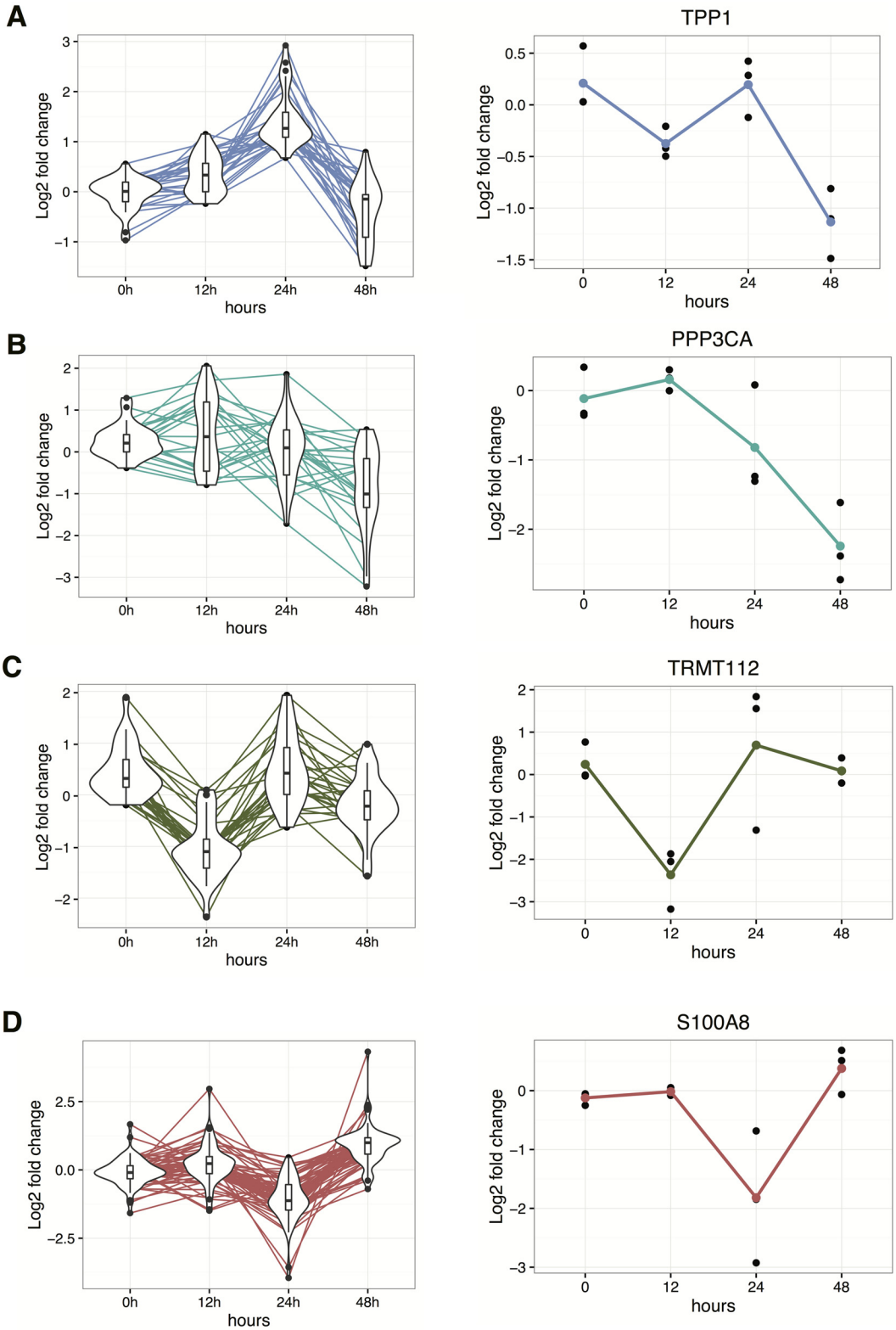

FIG. 3. **Traces and representative single proteins of clusters.** Log2 fold changes of all traces of each cluster and a representative single protein from each cluster are plotted in matching colors to the cluster they represent. Each letter (*A–D*) represents one of the clusters from Fig. 2. The violin plots represent the distribution of log2 fold change of every protein within the cluster. In the single protein figures, the *black dots* represent single measurements; the *colored dots* represent the mean of the log2 fold changes.

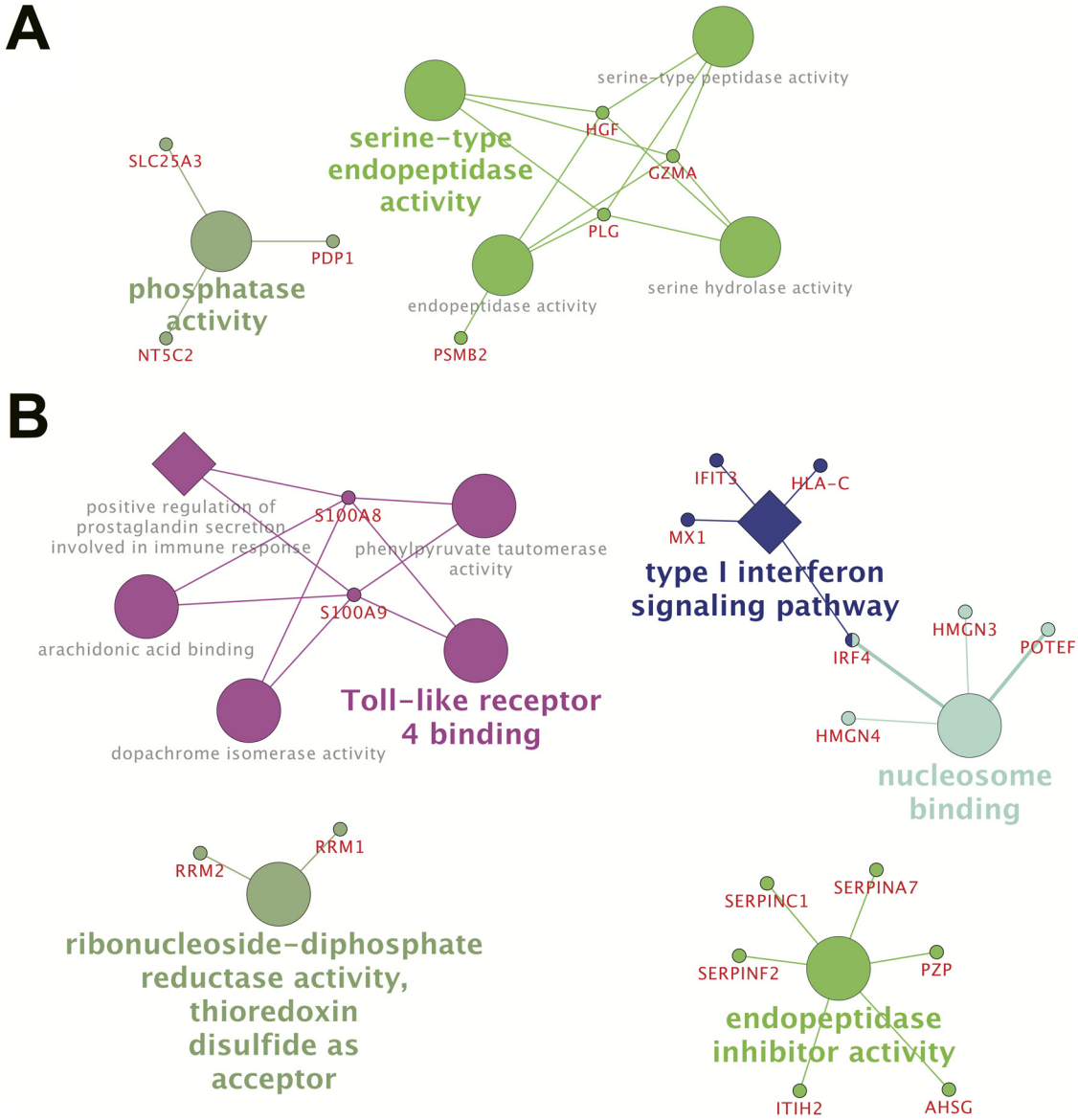

FIG. 4. **Functional annotation of the cluster analysis.** *A* and *B,* network of significantly enriched functional annotation terms of down-regulated proteins from cluster a (48 h after infection) and cluster b (24 h after infection), respectively. The GO terms immune system process (*diamond*) and molecular function (*ellipse*) were assessed using the GO term fusion function from the ClueGO Cytoscape plugin. *Different colors* were used for different functional groups. After network analysis of functional terms, the proteins underlying the significantly enriched functional term were added (protein names are in *red*). The protein library was used as reference data set. Significance was assessed using a two-sided hypergeometric test with a Bonferroni step down procedure to adjust for multiple testing.

are producer of TAP-1 and TAP-2 and are known to express CD4 when isolated from blood from human individuals (34). Hence, a negative sorting approach may be more suitable for this type of analysis. Among the down-regulated proteins, no significant enrichment of GO terms was detectable.

Comparison of in Vitro Infected CD4+ T Cells and CD4+ T Cells Sorted from Patients—Next, we aimed to compare *in vitro* infected CD4+ T cells and CD4+ T cells from patients. In a first step, we compared how the detected proteome of the two cell populations overlaps (Fig. 7*A*). 829 proteins were detected both *in vivo* and *in vitro*. Then, we compared all proteins considered to be significantly differentially regulated in both groups (Fig. 7*B*). The overlap was low with only 11 proteins changing both *in vivo* and *in vitro*. To assess whether this lack of overlap was due to the fact that the main changes were in proteins that were only detected in one of the groups, we compared all the proteins considered different in the two groups with the total of proteins detected in both groups (*overlap*, Fig. 7*C*). In the *in vitro* experiment, 97 proteins were considered different, which were not detected in the *in vivo* samples, whereas 37 proteins considered to be regulated in the *in vitro* time course were detected and considered as

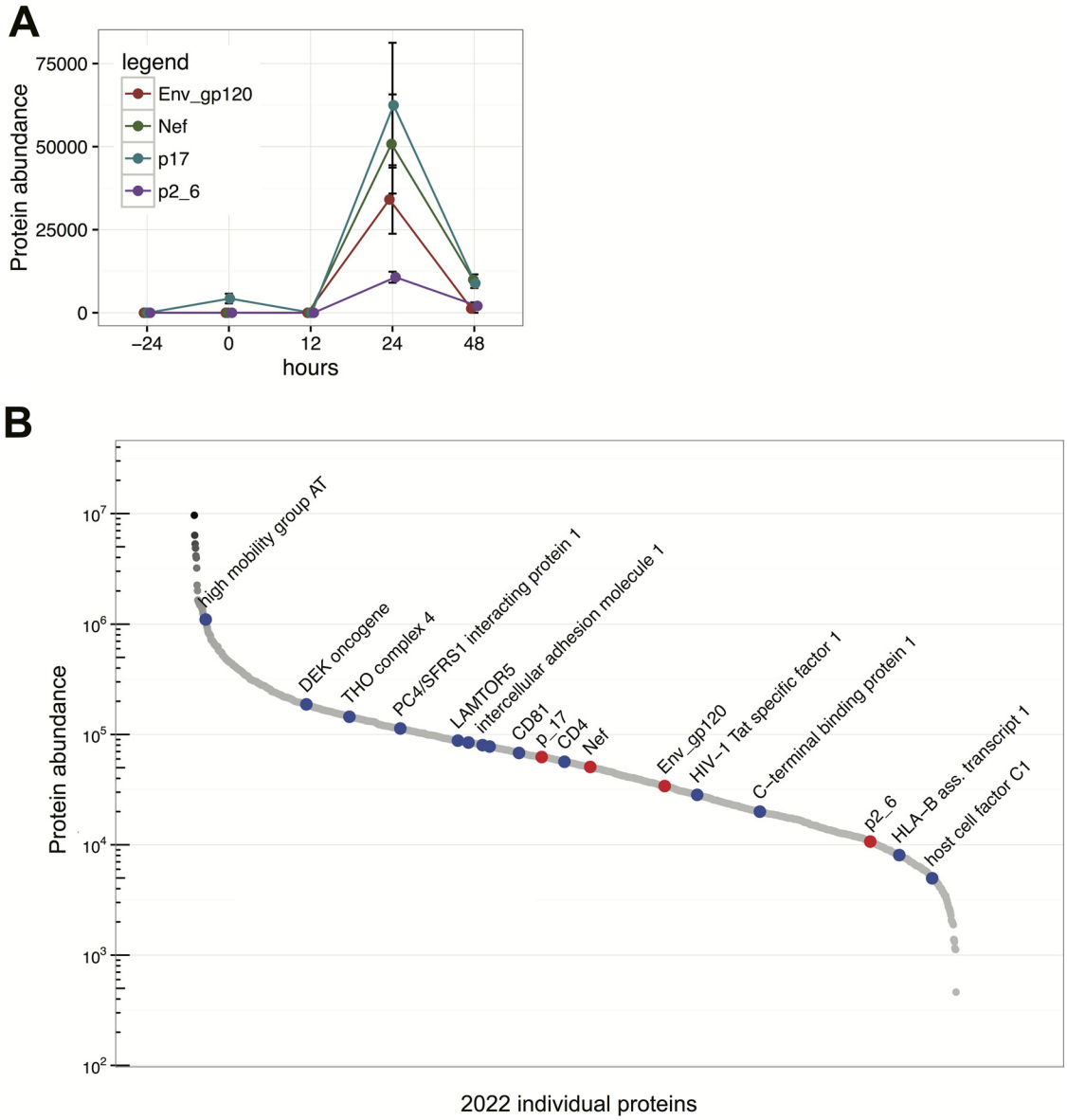

FIG. 5. **Analysis of detected HIV-1 proteins.** *A,* estimated abundances of HIV-1 proteins in CD4+ T cells over time as assessed by aLFQ. *B,* dynamic range of HIV-1 protein quantification within the whole proteome of CD4+ T cells after 24 h. The log10 abundance of all proteins detected is plotted. HIV-1 proteins are highlighted in *red*, human proteins of the functional GO term viral defense are highlighted in *blue*.

unchanged in the *in vivo* samples. Conversely, in the *in vivo* samples 14 proteins were considered different, which were not detected in the *in vitro* samples, whereas 147 proteins which were differentially regulated in the *in vivo* samples were detected and did not change in the *in vitro* time course. Hence, of the proteins that were detected in both sample types some overlap in differential expression was observed; however, the majority of proteins that were differentially expressed *in vitro* did not change *in vivo* and vice versa.

Functional enrichment analysis showed significant enrichment of type 1 interferon signaling in both *in vitro* infected CD4+ T cells as well as CD4+ T cells from patients. 4 and 5 proteins *in vitro* and *in vivo*, respectively, were significantly enriched for the GO term "type 1 interferon signaling" (Figs. 4*B* and 6*C*). A network based on published interactions using evidence based only on experiments and databases from STRING confirmed that the proteins are interacting based on experimentally observed protein-protein interactions (Fig. 7*D*). However, the type 1 interferon pathway is a central pathway in innate and adaptive immunity. Furthermore, type 1 interferon signaling may have both protective or detrimental effects for the host, depending on the timing, the state of the cell, and the cellular milieu (35). Consequently, assessing functionality based on the broad GO term "type 1 interferon signaling" might be an oversimplification. Therefore, we plotted the sig-

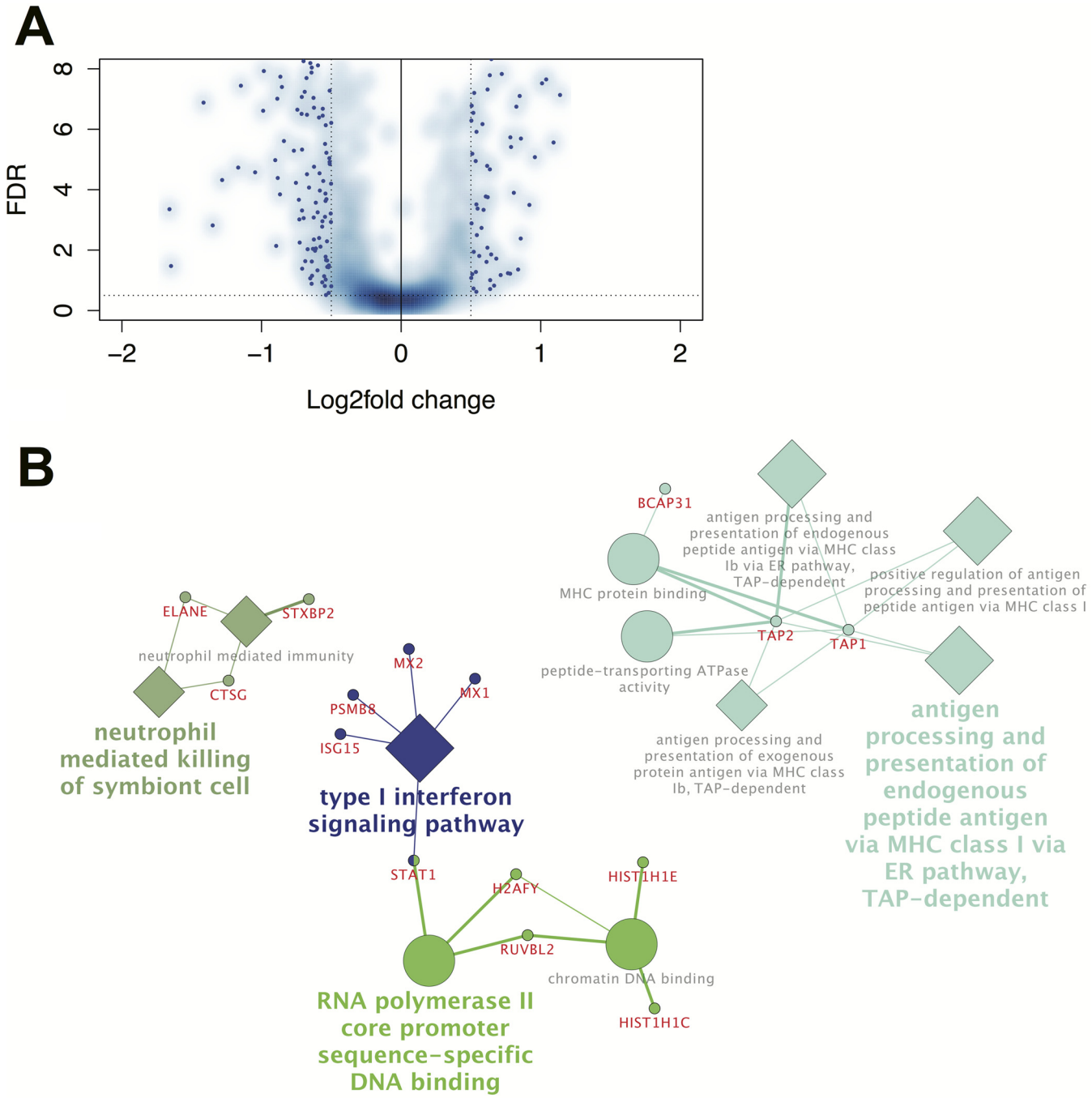

FIG. 6. **Qualitative and quantitative assessment of the proteome of human CD4+ T cells.** *A, volcano plot* showing log2 fold change of protein abundance plotted against −log10 adjusted *p* value for CD4+ T cells from viremic patients *versus* the same viremic patient. Data points *highlighted in blue* in the *upper right section* represent proteins that display an enrichment in of log2 fold change >0.5 and adjusted *p* value <0.05. A total of seven patients was assessed for this comparison. *B,* network of significantly enriched functional annotation terms of proteins from up-regulated proteins comparing the same patient during viremia and after successful treatment. The GO terms "immune system process" (*diamond*) and "molecular function" (*large circle*) were assessed using the GO term "fusion function" from the ClueGO package. *Different colors* were used for different functional groups. After network analysis of functional terms, the proteins underlying the significantly enriched functional term were added (*small circle,* protein names are in *red*). The protein list from the spectral library was used as reference data set. Significance was assessed using a two-sided hypergeometric test with a Bonferroni step down procedure to adjust for multiple testing.

nificantly enriched proteins within a diagram of interferon α/β signaling obtained from the REACTOME database (Fig. 8, *A* and *B*) (36). In direct comparison, differentially regulated proteins *in vivo* affect primarily proteins activating STAT-1, including STAT-1 itself; in turn, differentially regulated proteins *in vitro* are located downstream of STAT-1 activation in the

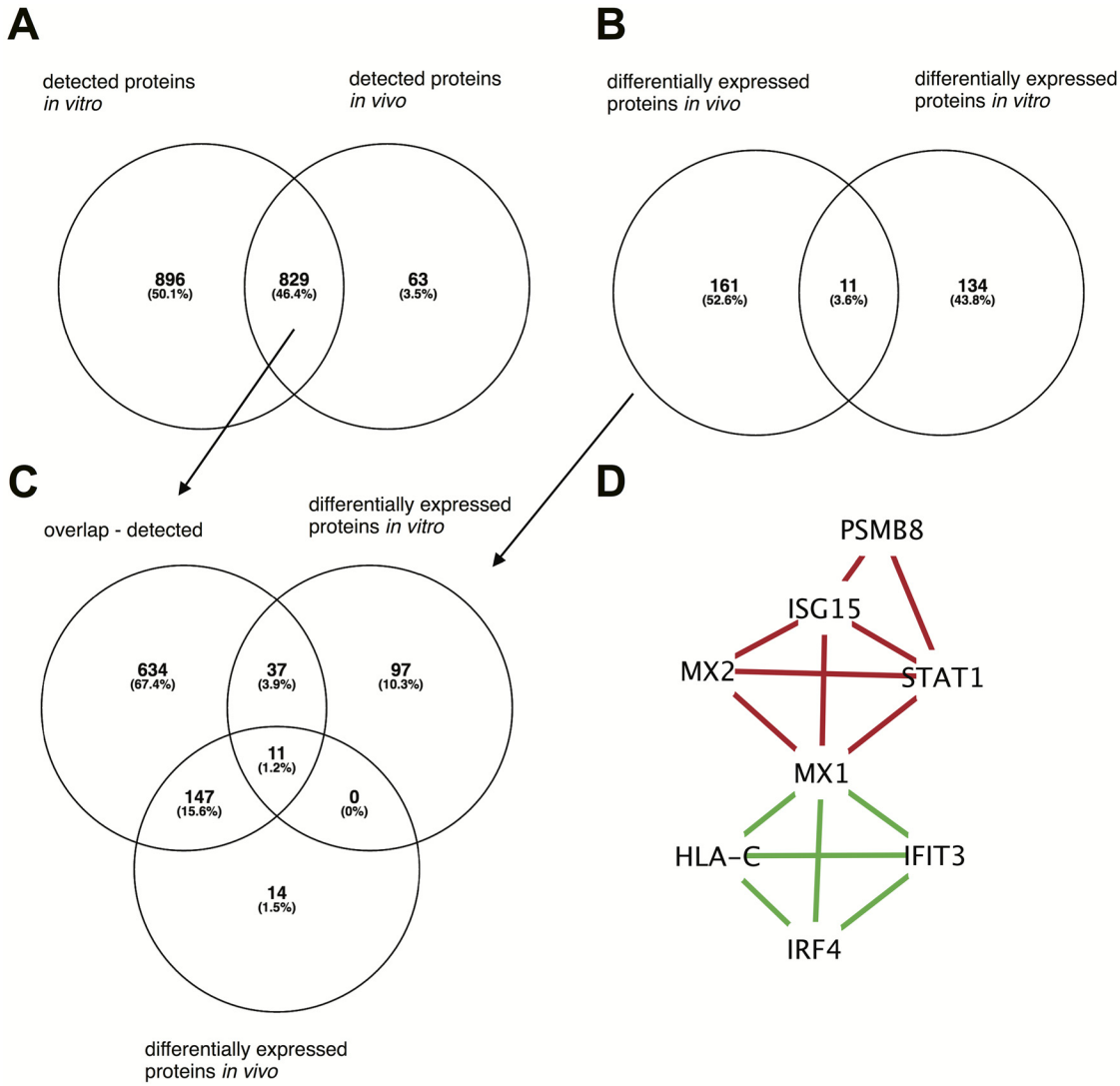

FIG. 7. **Comparison of the proteome of CD4+ T cells from the *in vitro* infection and from patients.** *A,* Venn diagram of all proteins detected in sorted CD4+ T cells in the *in vitro* infection experiment and CD4+ T cells from patients. *B,* Venn diagram of all significantly regulated proteins detected in sorted CD4+ T cells in the *in vitro* infection experiment and CD4+ T cells from patients. *C,* Venn diagram comparing the proteins found in both the *in vitro* and the *in vivo* experiments with the proteins that were regarded as significantly regulated in the *in vitro* infection experiment and in CD4+ T cells from patients. *D,* significantly enriched proteins from the network analysis in Figs. 4 and 6 plotted as STRING network using a confidence cutoff of 0.4, including interactions obtained from experiments and curated databases only. Nodes connected by *red edges* represent proteins from the *in vitro* experiment; nodes connected by *green edges* represent proteins from the *in vivo* experiment.

pathway, such as mediators of an antiviral state like IRF-4. Hence, despite the significant enrichment of the GO term type 1 interferon signaling *in vivo* and *in vitro*, the actual proteins may be different as well as their biological function (35). In sum, there is little overlap between the specific changes in the proteome comparing *in vivo* and *in vitro* infected CD4+ T cells but rather convergence at the pathway level of type 1 interferon signaling.

DISCUSSION

We examined the changes in the proteome of human CD4+ T cells associated with HIV-1 infection both *in vitro* and *in vivo*. The most profound changes in the overall proteome of CD4+ T cells infected with HIV-1 *in vitro* were detected 24 h after infection and involved important functional groups within the cell. In addition, we could measure the abundance and dynamics of certain HIV-1 proteins within the host proteome. Finally, we could reiterate some of the findings from the *in vitro* model using CD4+ T cells from HIV-1-infected individuals.

The proteome of *in vitro* HIV-1-infected human T cells has not been measured yet. Here, we present data from a comprehensive set of samples with longitudinal *in vitro* and *in vivo* samples. In addition, we could detect viral proteins, which

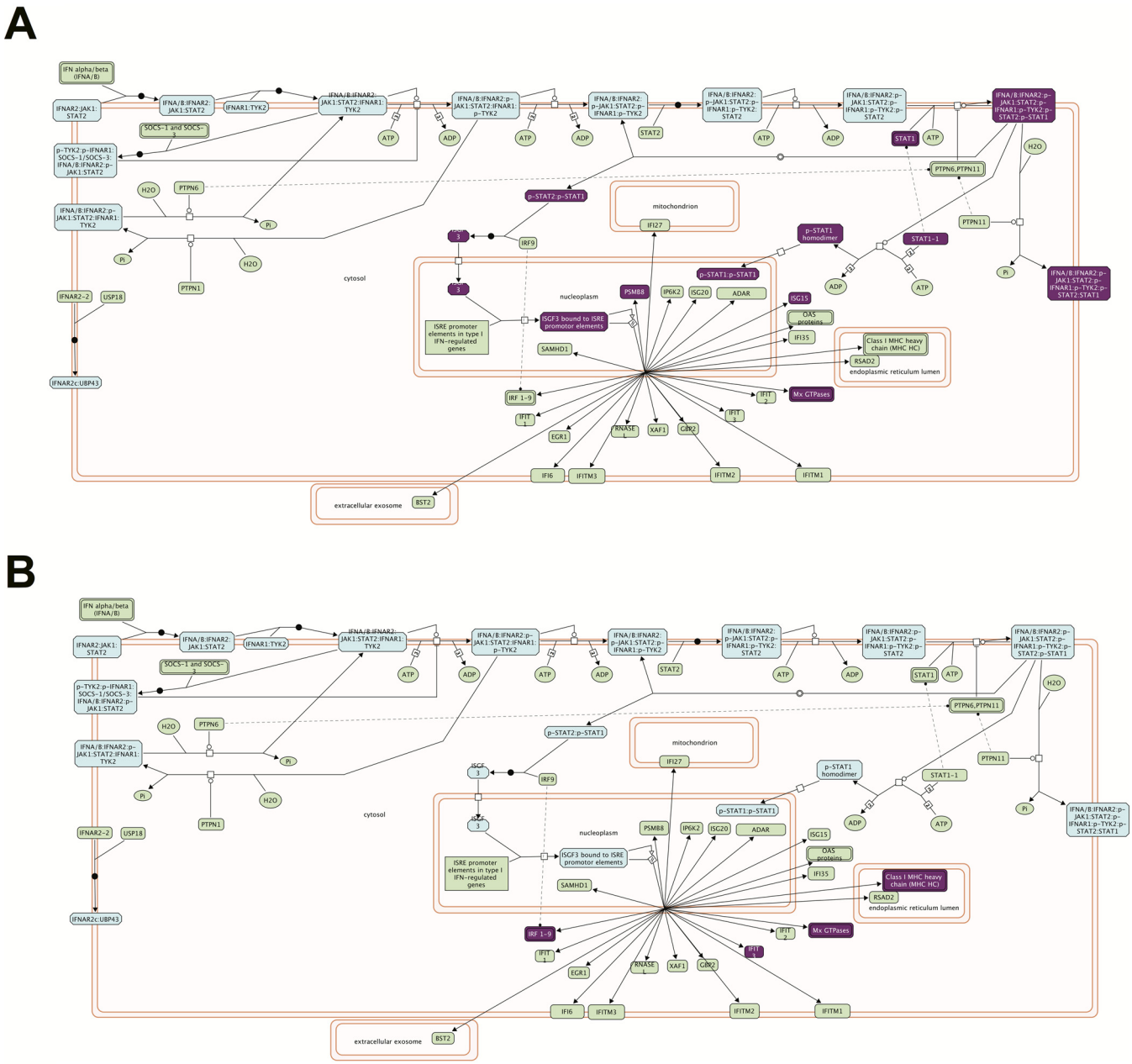

FIG. 8. **REACTOME diagrams of the type 1 interferon signaling pathway with highlighted and regulated proteins from the *in vivo* and *in vitro* experiments.** *A,* REACTOME diagram of the type 1 interferon signaling pathway highlighted (in *purple*), with differentially regulated proteins in CD4+ T cells from patients on and off treatment. *B,* REACTOME diagram of the type 1 interferon signaling pathway with highlighted (in *purple*) and differentially regulated proteins in CD4+ T cells infected *in vitro* at the 24-h time point.

enables us to put them in the context of the host proteome. A strength of our approach is the paired approach for both *in vitro* and *in vivo* samples. By comparing cells from the same donor or the same individuals at different time points, we can reduce inter-individual differences.

During the *in vitro* infection time course, changes in the CD4+ T cell proteome were most prominent 24 h after infection, simultaneous with the peak of viral protein production. GO term enrichment of immune system processes showed a decrease of proteins associated with TLR-4 signaling and type 1 interferon signaling. TLR-4 signaling has been shown to be an important regulator of T cell receptor signaling in T cells from mice (37). Conversely, the HIV-1 envelope protein gp120 has been shown to bind to TLR-4 (38). Our investigation shows a strong time-dependent association of decreased TLR-4 signaling and increased gp120 in the *in vitro* experiment.

Type 1 interferon signaling plays a central role in viral infections and has pleiotropic effects. Depending on the biological context, type 1 interferons may promote or inhibit T cell

activation, proliferation, differentiation, and survival (35). This central role may explain that we could detect changes in proteins associated with type 1 interferons both *in vitro* and *in vivo*.

Our enrichment analysis used the protein library only. Therefore, the number of proteins being enriched appears on first sight to be rather low. However, because the number of proteins in our custom protein library for a given GO term is limited, the enrichment is significant even with a low total amount of proteins. For example, four proteins linked to the GO term type 1 interferon changed in the *in vitro* experiment. The total number of proteins in our library linked to type 1 interferon is 31. Therefore, four changing proteins accounts for ~13% of all type 1 interferon-associated proteins, which is significant.

Our proteome approach and the re-discovery of certain proteins in the context of the whole proteome may be used to support results from genome analyses and put them into biological context. A recent meta-analysis of host cell genes involved in HIV-1 infection emphasized the importance of networks around STAT-1 (39), in line with our *in vivo* results. Hence, our proteome approach introduces not only an additional level of evidence on the proteome level *in vitro* but also re-emphasizes and highlights the role of these proteins in actual human individuals.

In addition to host proteins, we could directly detect HIV proteins in the *in vitro* time course. To the best of our knowledge, we are the first ones to report HIV proteins within the human proteome outside of protein-protein interactions studies (40). We could detect the most abundant late proteins at time point 24 h. The 12-h time may have been too early for the early HIV proteins, such as Tat and Rev (6). The other viral proteins might be expressed at insufficient levels for detection using our single-shot analysis method. This obstacle could be overcome by infecting a more susceptible T cell line that is known to produce much more HIV-1 proteins (5). However, in this study, we focused deliberately on primary CD4$^+$ T cells and clinical samples to assess the translational potential of SWATH-MS. CD4$^+$ T cells produced a significant amount of HIV-1 proteins within 24 h. In this experimental setting, we measure the overall protein production within the CD4$^+$ T cell population, which consists of infected and uninfected T cells. Therefore, from a single cell perspective, the total amount of HIV-1 protein produced is likely to be diluted and very likely to be higher than our estimate, although we tried to minimize the number of uninfected cells by using a multiplicity of infection of 1 in combination with spinoculation to synchronize the infection and enhance the infection rate, *i.e.* theoretically, each cell should be infected by HIV-1. However, not every primary CD4$^+$ T cell is, even after maximal stimulation, susceptible for HIV-1 infection *in vitro* (41).

Our results differ to some extent from previous data published on the proteome of *in vitro* infected T cell lines (7, 42). The study of Chan *et al.* found changes in 21% of proteins upon HIV infection. However, because T cell lines used are hyper-susceptible for HIV infection compared with human samples, direct comparison to our results is difficult.

Next, we assessed paired CD4$^+$ T cells from patients on and off treatment. Nevertheless, the differences in CD4$^+$ T cells were most pronounced between viremic and non-viremic patients. Whether this is a sampling bias or a real biological phenomenon remains unclear. However, it is tempting to speculate that as CD4$^+$ T cells are the main reservoir of HIV-1 in peripheral blood, they are most prone to changes upon treatment. The number of proteins detected from the clinical samples was low compared with cell lines but was comparable with other clinical tissues (43) and similar to a previous study that analyzed PBMCs by SWATH-MS (44). As such, optimization of the sample preparation from patient-derived PBMCs, combined with a deeper coverage in the spectral library via fractionation, may yield improved proteome coverage in future studies. A further limitation of the *in vivo* component of our study was the relatively limited numbers of patient samples analyzed, which resulted in a relatively low number of proteins called as differentially expressed likely reflecting the large differences in genetic and environmental backgrounds of the patients. Hence, because of the heterogeneity of data, the patient samples represent a pilot analysis, and a larger number of samples is required for more statistical power to overcome strongly confounding signals not related to the viral infection.

Even though we used primary human CD4$^+$ T cells for the *in vitro* infection, it is difficult to compare these findings directly to the changes detected in the proteome of patients during HIV-1 infection. First and foremost, the relationship of infected *versus* bystander cells is fundamentally different. *In vitro*, we expect a high percentage of infected cells, whereas *in vivo* the overwhelming majority of cells is not infected (41). In addition, for an *in vitro* infection of human CD4$^+$ T cells to be successful, the cells must be artificially activated. Hence, the *in vitro* data in our investigation display the changes within the proteome against a strong background of activation. We tried to be as specific as possible to detect only changes associated with HIV-1 by comparing activated and simultaneously HIV-1-infected cells against activated cells only at the same time points. This approach notwithstanding, the detectable changes are still against a background of high activation. In humans, in contrast, inflammation is associated with viremia; suppression of viremia, in turn, abrogates inflammation. Hence, the reported comparison of T cells from viremic *versus* non-viremic patients includes changes attributable to resolving inflammation as well. Furthermore, the changes detectable over time in the *in vitro* system with a defined infection time point are likely to occur at the same time in an infected individual, for example, infection, integration, and assembly of the virus are likely to happen constantly in humans and successively *in vitro*. Finally, differences in the host (such as genetic differences, differences within the virus, and differences in the handling of clinical samples) contribute to

increase the noise within the measurements. Despite all these drawbacks, we could link changes in the proteome both *in vivo* and *in vitro*, for example with proteins associated with type 1 interferon signaling. However, it is worth noting that there may be relevant biological differences in the differentially expressed proteins associated with the GO term "type 1 interferon signaling" in the *in vivo* and the *in vitro* samples.

In sum, we analyzed the changes of the proteome of human CD4+ T cells associated with HIV-1 infection in both an *in vitro* model of infection and cells derived from HIV-1-infected patients. To our best knowledge, the proteome of CD4+ T cells from HIV-infected humans has not been measured before. Our results warrant further studies with larger patient numbers and different clinical end points to better understand the host immune system in HIV-1 infection.

Acknowledgments—We thank the patients participating in the ZPHI study and Ch. Grube and the physicians for excellent patient care. The following reagent was obtained through the AIDS Reagent Program, Division of AIDS, NIAID, National Institutes of Health, pJR-FL from Dr. Irvin Chen (46–48).

This work is dedicated to the memory of Franz Peter Oesch, 1/19/1943 to 8/15/2015.

DATA AVAILABILITY

The mass spectrometry proteomics data has been deposited to the ProteomeXchange Consortium (http://proteomecentral.proteomexchange.org) via the PRIDE partner repository (45) with the data set identifier PXD005234.

* The ZPHI study is supported by the clinical research Priority Program of the University of Zurich "Viral Infectious Diseases, ZPHI" (to H. F. G.). The authors declare that they have no conflicts of interest with the contents of this article. The content is solely the responsibility of the authors and does not necessarily represent the official views of the National Institutes of Health.

S This article contains supplemental material.

¶ Supported by the Swiss Foundation for Excellence and Talent in Biomedical Research.

‡‡ To whom correspondence should be addressed: collins@imsb.biol.ethz.ch or huldrych.guenthard@usz.ch.

§§ Supported by Swiss National Science Foundation Ambizione Grant PZ00P3_161435.

REFERENCES

1. Günthard, H. F., Saag, M. S., Benson, C. A., del Rio, C., Eron, J. J., Gallant, J. E., Hoy, J. F., Mugavero, M. J., Sax, P. E., Thompson, M. A., Gandhi, R. T., Landovitz, R. J., Smith, D. M., Jacobsen, D. M., and Volberding, P. A. (2016) Antiretroviral drugs for treatment and prevention of HIV infection in adults: 2016 recommendations of the International Antiviral Society-U.S.A. Panel. *JAMA* **316,** 191–210
2. Vandergeeten, C., Fromentin, R., DaFonseca, S., Lawani, M. B., Sereti, I., Lederman, M. M., Ramgopal, M., Routy, J.-P., Sékaly, R.-P., and Chomont, N. (2013) Interleukin-7 promotes HIV persistence during antiretroviral therapy. *Blood* **121,** 4321–4329
3. Virgin, H. W., and Walker, B. D. (2010) Immunology and the elusive AIDS vaccine. *Nature* **464,** 224–231
4. Fauci, A. S., Folkers, G. K., and Marston, H. D. (2014) Ending the global HIV/AIDS pandemic: the critical role of an HIV vaccine. *Clin. Infect. Dis.* **59,** S80–S84
5. Mohammadi, P., Desfarges, S., Bartha, I., Joos, B., Zangger, N., Muñoz, M., Günthard, H. F., Beerenwinkel, N., Telenti, A., and Ciuffi, A. (2013) 24 hours in the life of HIV-1 in a T cell line. *PLoS Pathog.* **9,** e1003161
6. Holmes, M., Zhang, F., and Bieniasz, P. D. (2015) Single-cell and single-cycle analysis of HIV-1 replication. *PLoS Pathog.* **11,** e1004961
7. Navare, A. T., Sova, P., Purdy, D. E., Weiss, J. M., Wolf-Yadlin, A., Korth, M. J., Chang, S. T., Proll, S. C., Jahan, T. A., Krasnoselsky, A. L., Palermo, R. E., and Katze, M. G. (2012) Quantitative proteomic analysis of HIV-1-infected CD4+ T cells reveals an early host response in important biological pathways: protein synthesis, cell proliferation, and T-cell activation. *Virology* **429,** 37–46
8. Haverland, N. A., Fox, H. S., and Ciborowski, P. (2014) Quantitative proteomics by SWATH-MS reveals altered expression of nucleic acid binding and regulatory proteins in HIV-1-infected macrophages. *J. Proteome Res.* **13,** 2109–2119
9. Fellay, J., Ge, D., Shianna, K. V., Colombo, S., Ledergerber, B., Cirulli, E. T., Urban, T. J., Zhang, K., Gumbs, C. E., Smith, J. P., Castagna, A., Cozzi-Lepri, A., De Luca, A., Easterbrook, P., Günthard, H. F., *et al.* (2009) Common genetic variation and the control of HIV-1 in humans. *PLoS Genet.* **5,** e1000791
10. Fraser, C., Lythgoe, K., Leventhal, G. E., Shirreff, G., Hollingsworth, T. D., Alizon, S., and Bonhoeffer, S. (2014) Virulence and pathogenesis of HIV-1 infection: an evolutionary perspective. *Science* **343,** 1243727
11. Rotger, M., Dang, K. K., Fellay, J., Heinzen, E. L., Feng, S., Descombes, P., Shianna, K. V., Ge, D., Günthard, H. F., Goldstein, D. B., Telenti, A., Swiss HIV Cohort Study, and the Center for HIV/AIDS Vaccine Immunology (2010) Genome-wide mRNA expression correlates of viral control in CD4+ T-cells from HIV-1-infected individuals. *PLoS Pathog.* **6,** e1000781
12. Sedaghat, A. R., German, J., Teslovich, T. M., Cofrancesco, J., Jr., Jie, C. C., Talbot, C. C., Jr., and Siliciano, R. F. (2008) Chronic CD4+ T-cell activation and depletion in human immunodeficiency virus type 1 infection: type I interferon-mediated disruption of T-cell dynamics. *J. Virol.* **82,** 1870–1883
13. Aebersold, R., and Mann, M. (2016) Mass-spectrometric exploration of proteome structure and function. *Nature* **537,** 347–355
14. Röst, H. L., Rosenberger, G., Navarro, P., Gillet, L., Miladinović, S. M., Schubert, O. T., Wolski, W., Collins, B. C., Malmström, J., Malmström, L., and Aebersold, R. (2014) OpenSWATH enables automated, targeted analysis of data-independent acquisition MS data. *Nat. Biotechnol.* **32,** 219–223
15. Gillet, L. C., Navarro, P., Tate, S., Röst, H., Selevsek, N., Reiter, L., Bonner, R., and Aebersold, R. (2012) Targeted data extraction of the MS/MS spectra generated by data-independent acquisition: a new concept for consistent and accurate proteome analysis. *Mol. Cell. Proteomics* **11,** O111.016717
16. Collins, B. C., Hunter, C. L., Liu, Y., Schilling, B., Rosenberger, G. R., Bader, S. L., Chan, D. W., Gibson, B. W., Gingras, A.-C., Held, J. M., Hirayama-Kurogi, M., Hou, G., Krisp, C. K., Larsen, B., Lin, L., Liu, S., Molloy, M. P., Moritz, R. L., Ohtsuki, S., Schlapbach, R., Selevsek, N., Thomas, S. N., Tzeng, S.-C., Zhang, H., and Aebersold, R. (2016) Multi-laboratory assessment of reproducibility, qualitative and quantitative performance of SWATH-mass spectrometry. bioRxiv, 074567, https://doi.org/10.1101/074567
17. Rieder, P., Joos, B., Scherrer, A. U., Kuster, H., Braun, D., Grube, C., Niederöst, B., Leemann, C., Gianella, S., Metzner, K. J., Böni, J., Weber, R., and Günthard, HF. (2011) Characterization of human immunodeficiency virus type 1 (HIV-1) diversity and tropism in 145 patients with primary HIV-1 infection. *Clin. Infect. Dis.* **53,** 725–731
18. Althaus, C. F., Vongrad, V., Niederöst, B., Joos, B., Di Giallonardo, F., Rieder, P., Pavlovic, J., Trkola, A., Günthard, H. F., Metzner, K. J., and Fischer, M. (2012) Tailored enrichment strategy detects low abundant small noncoding RNAs in HIV-1-infected cells. *Retrovirology* **9,** 27
19. Rusert, P., Fischer, M., Joos, B., Leemann, C., Kuster, H., Flepp, M., Bonhoeffer, S., Günthard, H. F., and Trkola, A. (2004) Quantification of infectious HIV-1 plasma viral load using a boosted *in vitro* infection protocol. *Virology* **326,** 113–129
20. Schubert, O. T., Gillet, L. C., Collins, B. C., Navarro, P., Rosenberger, G., Wolski, W. E., Lam, H., Amodei, D., Mallick, P., MacLean, B., and Aebersold, R. (2015) Building high-quality assay libraries for targeted analysis of SWATH MS data. *Nat. Protoc.* **10,** 426–441

21. Giallonardo, F. D., Töpfer, A., Rey, M., Prabhakaran, S., Duport, Y., Leemann, C., Schmutz, S., Campbell, N. K., Joos, B., Lecca, M. R., Patrignani, A., Däumer, M., Beisel, C., Rusert, P., Trkola, A., *et al.* (2014) Full-length haplotype reconstruction to infer the structure of heterogeneous virus populations. *Nucleic Acids Res.* **42,** e115
22. Röst, H. L., Liu, Y., D'Agostino, G., Zanella, M., Navarro, P., Rosenberger, G., Collins, B. C., Gillet, L., Testa, G., Malmström, L., and Aebersold, R. (2016) TRIC: an automated alignment strategy for reproducible protein quantification in targeted proteomics. *Nat. Methods* **13,** 777–783
23. Rosenberger, G., Ludwig, C., Röst, H. L., Aebersold, R., and Malmström, L. (2014) aLFQ: an R-package for estimating absolute protein quantities from label-free LC-MS/MS proteomics data. *Bioinformatics* **30,** 2511–2513
24. Bindea, G., Mlecnik, B., Hackl, H., Charoentong, P., Tosolini, M., Kirilovsky, A., Fridman, W.-H., Pagès, F., Trajanoski, Z., and Galon, J. (2009) ClueGO: a Cytoscape plug-in to decipher functionally grouped gene ontology and pathway annotation networks. *Bioinformatics* **25,** 1091–1093
25. Josefsson, L., King, M. S., Makitalo, B., Brännström, J., Shao, W., Maldarelli, F., Kearney, M. F., Hu, W.-S., Chen, J., Gaines, H., Mellors, J. W., Albert, J., Coffin, J. M., and Palmer, S. E. (2011) Majority of CD4+ T cells from peripheral blood of HIV-1-infected individuals contain only one HIV DNA molecule. *Proc. Natl. Acad. Sci. U.S.A.* **108,** 11199–11204
26. Teo, G., Kim, S., Tsou, C.-C., Collins, B., Gingras, A.-C., Nesvizhskii, A. I., and Choi, H. (2015) mapDIA: Preprocessing and statistical analysis of quantitative proteomics data from data independent acquisition mass spectrometry. *J. Proteomics* **129,** 108–120
27. Schubert, O. T., Ludwig, C., Kogadeeva, M., Zimmermann, M., Rosenberger, G., Gengenbacher, M., Gillet, L. C., Collins, B. C., Röst, H. L., Kaufmann, S. H., Sauer, U., and Aebersold, R. (2015) Absolute proteome composition and dynamics during dormancy and resuscitation of *Mycobacterium tuberculosis*. *Cell Host Microbe* **18,** 96–108
28. Stumptner-Cuvelette, P., Morchoisne, S., Dugast, M., Le Gall, S., Raposo, G., Schwartz, O., and Benaroch, P. (2001) HIV-1 Nef impairs MHC class II antigen presentation and surface expression. *Proc. Natl. Acad. Sci. U.S.A.* **98,** 12144–12149
29. Muratori, C., Cavallin, L. E., Krätzel, K., Tinari, A., De Milito, A., Fais, S., D'Aloja, P., Federico, M., Vullo, V., Fomina, A., Mesri, E. A., Superti, F., and Baur, A. S. (2009) Massive secretion by T cells is caused by HIV Nef in infected cells and by Nef transfer to bystander cells. *Cell Host Microbe* **6,** 218–230
30. Okumura, A., Lu, G., Pitha-Rowe, I., and Pitha, P. M. (2006) Innate antiviral response targets HIV-1 release by the induction of ubiquitin-like protein ISG15. *Proc. Natl. Acad. Sci. U.S.A.* **103,** 1440–1445
31. Scagnolari, C., Monteleone, K., Selvaggi, C., Pierangeli, A., D'Ettorre, G., Mezzaroma, I., Turriziani, O., Gentile, M., Vullo, V., and Antonelli, G. (2016) ISG15 expression correlates with HIV-1 viral load and with factors regulating T cell response. *Immunobiology* **221,** 282–290
32. Yeung, M. L., Houzet, L., Yedavalli, V. S., and Jeang, K.-T. (2009) A genome-wide short hairpin RNA screening of Jurkat T-cells for human proteins contributing to productive HIV-1 replication. *J. Biol. Chem.* **284,** 19463–19473
33. Mu, X., Fu, Y., Zhu, Y., Wang, X., Xuan, Y., Shang, H., Goff, S. P., and Gao, G. (2015) HIV-1 exploits the host factor RuvB-like 2 to balance viral protein expression. *Cell Host Microbe* **18,** 233–242
34. O'Doherty, U., Steinman, R. M., Peng, M., Cameron, P. U., Gezelter, S., Kopeloff, I., Swiggard, W. J., Pope, M., and Bhardwaj, N. (1993) Dendritic cells freshly isolated from human blood express CD4 and mature into typical immunostimulatory dendritic cells after culture in monocyte-conditioned medium. *J. Exp. Med.* **178,** 1067–1076
35. Crouse, J., Kalinke, U., and Oxenius, A. (2015) Regulation of antiviral T cell responses by type I interferons. *Nat. Rev. Immunol.* **15,** 231–242
36. Fabregat, A., Sidiropoulos, K., Garapati, P., Gillespie, M., Hausmann, K., Haw, R., Jassal, B., Jupe, S., Korninger, F., McKay, S., Matthews, L., May, B., Milacic, M., Rothfels, K., Shamovsky, V., Webber, M., Weiser, J., Williams, M., Wu, G., Stein, L., Hermjakob, H., and D'Eustachio, P. (2016) The reactome pathway knowledgebase. *Nucleic Acids Res.* **44,** D481–D487
37. González-Navajas, J. M., Fine, S., Law, J., Datta, S. K., Nguyen, K. P., Yu, M., Corr, M., Katakura, K., Eckman, L., Lee, J., and Raz, E. (2010) TLR4 signaling in effector CD4+ T cells regulates TCR activation and experimental colitis in mice. *J. Clin. Invest.* **120,** 570–581
38. Ben Haij, N., Leghmari, K., Planès, R., Thieblemont, N., and Bahraoui, E. (2013) HIV-1 Tat protein binds to TLR4-MD2 and signals to induce TNF-α and IL-10. *Retrovirology* **10,** 123
39. Bushman, F. D., Malani, N., Fernandes, J., D'Orso, I., Cagney, G., Diamond, T. L., Zhou, H., Hazuda, D. J., Espeseth, A. S., König, R., Bandyopadhyay, S., Ideker, T., Goff, S. P., Krogan, N. J., Frankel, A. D., *et al.* (2009) Host cell factors in HIV replication: meta-analysis of genome-wide studies. *PLoS Pathog.* **5,** e1000437
40. Luo, Y., Jacobs, E. Y., Greco, T. M., Mohammed, K. D., Tong, T., Keegan, S., Binley, J. M., Cristea, I. M., Fenyö, D., Rout, M. P., Chait, B. T., and Muesing, M. A. (2016) HIV-host interactome revealed directly from infected cells. *Nat. Microbiol.* **1,** 16068
41. Ciuffi, A., Bleiber, G., Muñoz, M., Martinez, R., Loeuillet, C., Rehr, M., Fischer, M., Günthard, H. F., Oxenius, A., Meylan, P., Bonhoeffer, S., Trono, D., and Telenti, A. (2004) Entry and transcription as key determinants of differences in CD4 T-cell permissiveness to human immunodeficiency virus type 1 infection. *J. Virol.* **78,** 10747–10754
42. Chan, E. Y., Qian, W.-J., Diamond, D. L., Liu, T., Gritsenko, M. A., Monroe, M. E., Camp, D. G., 2nd., Smith, R. D., and Katze, M. G. (2007) Quantitative analysis of human immunodeficiency virus type 1-infected CD4+ cell proteome: dysregulated cell cycle progression and nuclear transport coincide with robust virus production. *J. Virol.* **81,** 7571–7583
43. Rosenberger, G., Koh, C. C., Guo, T., Röst, H. L., Kouvonen, P., Collins, B. C., Heusel, M., Liu, Y., Caron, E., Vichalkovski, A., Faini, M., Schubert, O. T., Faridi, P., Ebhardt, H. A., Matondo, M., Lam, H., Bader, S. L., Campbell, D. S., Deutsch, E. W., Moritz, R. L., Tate, S., and Aebersold, R. (2014) A repository of assays to quantify 10,000 human proteins by SWATH-MS. *Sci. Data* **1,** 140031
44. Silva, C., Santa, C., Anjo, S. I., and Manadas, B. (2016) A reference library of peripheral blood mononuclear cells for SWATH-MS analysis. *Proteomics* **10,** 760–764
45. Vizcaíno, J. A., Côté, R. G., Csordas, A., Dianes, J. A., Fabregat, A., Foster, J. M., Griss, J., Alpi, E., Birim, M., Contell, J., O'Kelly, G., Schoenegger, A., Ovelleiro, D., Pérez-Riverol, Y., Reisinger, F., Ríos, D., *et al.* (2013) The PRoteomics IDEntifications (PRIDE) database and associated tools: status in 2013. *Nucleic Acids Res.* **41,** D1063–D1069
46. O'Brien, W. A., Koyanagi, Y., Namazie, A., Zhao, J.-Q., Diagne, A., Idler, K., Zack, J. A., and Chen, I. S. (1990) HIV-1 tropism for mononuclear phagocytes can be determined by regions of gp120 outside the CD4-binding domain. *Nature* **348,** 69–73
47. Koyanagi, Y., Miles, S., Mitsuyasu, R. T., Merrill, J. E., Vinters, H. V., and Chen, I. S. (1987) Dual infection of the central nervous system by AIDS viruses with distinct cellular tropisms. *Science* **236,** 819–822
48. Koyanagi, Y., O'Brien, W. A., Zhao, J. Q., Golde, D. W., Gasson, J. C., and Chen, I. S. (1988) Cytokines alter production of HIV-1 from primary mononuclear phagocytes. *Science* **241,** 1673–1675